Reynolds Stress Tensor Measurements In A Shear-Thinning Fluid Using Magnetic Resonance Velocimetry: A Parameter Study With The FDA Benchmark Nozzle

Kristine John[1,*], Carolin Wüstenhagen[1], Martin Bruschewski[1], Sven Grundmann[1]

1: Institute of Fluid Mechanics, University of Rostock, Germany
*Corresponding author: kristine.john@uni-rostock.de

Keywords: magnetic resonance velocimetry, MRV, Reynolds stress tensor, non-Newtonian fluids, FDA benchmark nozzle

ABSTRACT

Compared to refractive index matching in laser optical measurement techniques, magnetic resonance velocimetry (MRV) is assumed to be comparatively robust to changes in fluid composition when the principal components of the mixture provide a measurable MRI signal. In previous studies, MRV measurements were performed with differ-ent mixtures of water and glycerol, and no significant errors arose regardless of the mixing ratio. MRV is therefore proposed as a promising method for providing experimental data for a wide range of fluids that may also replicate different viscosity models. However, MRV can suffer from so-called chemical shift artifacts caused by slight variations in resonance frequency of differently bound hydrogen protons. These effects may arise when additional components are added to the flow medium. In this study, the ability of MRV to measure different flow mixtures is investigated. The long-term goal is to provide comprehensive experimental validation data for viscosity models in numerical simulations. Measurements were performed in stationary fluid samples as well as in flow measurements at the sudden expansion of the FDA benchmark nozzel. It is shown that MRV can provide reliable results for a Newtonian fluid and a shear-thinning fluid.

1. Introduction

Numerical simulations of turbulent flows are essential for many applications. For example, detailed knowledge of the flow field is critical in developing medical implants that affect blood flow. The U.S. Food and Drug Administration (FDA) has presented a standardized procedure for evaluating numerical models (Stewart et al., 2013). They proposed a pipe with a continuous contraction followed by a sudden expansion and standardized boundary conditions as a test case that allow for the comparison of different turbulence models. The results were validated using experimental data from particle image velocimetry (PIV) performed in different laboratories and published by Hariharan et al. (2011). The flow medium used was Newtonian, which is often assumed to

be accurate enough for higher Reynolds numbers, but which does not properly reflect the shear-thinning properties of blood. Therefore, several studies have investigated the influence of different viscosity models on numerical results using the FDA benchmark. For example, Trias et al. (2014) simulated the flow through the sudden expansion using different viscosity models for Reynolds number 500 and found that the differences raise up to 10%. More recently, Hussein et al. (2021) explored a wider range of Reynolds numbers and compared the results for a Newtonian viscosity and the Carreau model. They also observed differences in the results, especially for low Reynolds numbers, while for higher Reynolds numbers, the flows seems similar. But, as far as the authors are aware, there is no comprehensive experimental study on the FDA nozzle to study the influence of non-Newtonian Effects on the flow field.

This study investigates the ability of MRV to provide experimental data for the FDA benchmark using magnetic resonance velocimetry (MRV) to validate viscosity models in numerical simulations. The technique allows two- or three-dimensional measurements of the three-component (3C) velocity vector and the six-component (6C) Reynolds Stress Tensor (RST). Moreover, it does not require optical access to the flow field or tracer particles. In an initial study on the benchmark nozzle, two-dimensional mean velocity measurements were used to validate numerical simulations (Konnigk et al., 2021). In another study by John et al. (2022), the results of velocity and RST measurements were compared to PIV data presented by Hariharan et al. (2011). They showed good agreement for both measurement methods concerning the velocity field, but systematic errors were visible in the MRV data for the RST measurement. However, the qualitative results agreed well with the data from optical measurements, and ways to further suppress these errors are part of ongoing research.

In previous studies, MRV measurements were performed with different Newtonian mixtures of water and glycerol without errors arising that could be attributed to depend on the fluid. MRV is therefore believed to be a promising method to also measure non-Newtonian fluids without major experimental difficulties. However, variations in resonance frequency of differently bound hydrogen protons may lead to so-called chemical shift artifacts when adding further components to the mixture. Therefore, this study investigates the ability of MRV to measure different flow mixtures to provide experimental validation data for viscosity models in numerical simulations.

2. Material and Methods

2.1. Experimental Setup

In the first measurement, different stationary fluids are measured, containing purified water and glycerol as the main components. In addition, some include xanthan gum to create shear thinning behavior and copper sulfate to improve the MRI signal. All samples were stirred for 12h with a magnetic stirrer to achieve homogeneous mixing. For a proof of concept, a Newtonian (NF) and a non-Newtonian (NNF) fluid were then used for flow measurements in the FDA nozzle to demonstrate the capabilities of MRV measurements with these different types of fluids. The NF

is composed of 50% glycerol and 50% purified water with a dynamic viscosity of η = 6.2 mPa·s and a density of $\rho = 1240$ kg/m^3. For the NNF, the water share is increased to 80%, and 0.05% of xanthan gum was added to obtain shear thinning behavior. The density of this mixture is $\rho = 1045$ kg/m^3.

The FDA nozzle model used in this study is enlarged 8.3 times to reach a higher relative resolution. The geometry of the nozzle was milled from polyoxymethylene (POM) and placed inside a pipe made from poly(methyl methacrylate) (PMMA). Both materials were described as having a susceptibility close to the one of water (Wapler et al., 2014) which minimizes the risk of material-induced measurement artifacts. A customized 32-channel receiving coil is placed around the region of interest to receive the MRI signal. A schematic of the FDA-Nozzle and its positioning inside the MRI examination room is displayed in fig. 1.

The setup is connected via flexible hoses to the flow-providing system outside of the MRI examination room. Both fluids were kept in a 300 l tank and pumped with an eccentric screw container pump (JP-700 DR, Jessberger, Ottobrunn bei München, Germany). The flow rate was measured using a magnetic-inductive sensor (IFM SM7200, ifm electronics, Essen, Germany). Two flow rates (Q=40 l/min and Q=50 l/min) were measured, corresponding to Reynolds numbers of approximately 5000 and 6500, respectively, for the Newtonian fluid. The rheological properties of the fluids were measured using an Anton Paar air-bearing rotation viscometer (MCR 702 TwinDrive, Anton Paar Germany GmbH, Ostfildern-Scharnhausen Germany). A 50 mm diameter cone-plate geometry with an angle of 1° and a gap of 0.098 mm is used for the measurements to ensure a constant shear rate over the fluid volume. The used rheometer has a minimum torque of 1 nNm. Thus, the minimum shear rate that can be applied depends on the fluid's viscosity. The shear rate was changed in logarithmic equidistant steps up to a maximum shear rate of 1000 1/s. All measurements were performed at 20 °C. Each sample was measured three times, and the results were averaged.

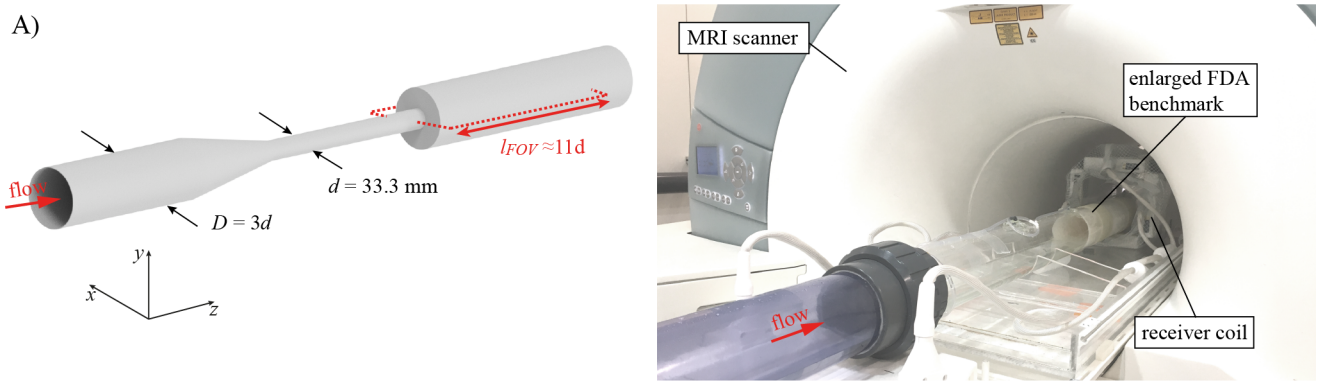

Figure 1. A) Schematic of the scaled FDA nozzle used in this study, B) positioning of the flow model insinde the MRI scanner.

Table 1. Measurement parameter

	2D3C velocity	2D6C RST
Orientation	coronal	coronal
Encoding	4-Point	ICOSA6
FOV (x, y, z) in mm	5,126,360	5,126,360
Matrix size (x, y, z)	1,84,240	1,84,240
TE/TR in ms	2.37/7.00	3.34/7.00
Flip angle in °	10	10
Bandwith in Hz/Px	1390	1390
M_1^{enc} in mT/m· ms^2	7.5	{10,12,15,20,30}
Readout direction	z	z
Number of averages	256	{150, 175, 200, 225, 250}

2.2. Magnetic Resonance Velocimetry

In MRV, the velocity vector and the Reynolds stress Tensor can be measured due to a correlation to the signals' phase angle and magnitude, respectively, at a known change in the first moment of the magnetic field gradient (M_1). Here, a custom velocity-encoded gradient recalled echo (GRE) sequence as applied in the previous study by John et al. (2022) was used. The velocity field was acquired using 4-Point imaging based on the method proposed by Markl et al. (2012), and six-directional icosahedral (ICOSA6) motion-encoding was used for turbulence quantification as described in Zwart & Pipe (2013) and Haraldsson et al. (2018). Recent studies using these encoding strategies and comparing the results with laser optical measurements showed promising results (John et al., 2022; Schmidt et al., 2021).

The data was acquired in a 360 mm long and 126 mm wide horizontal field of view (FOV) reaching approximately from one contraction diameter (d) upstream of the sudden expansion to $10\,d$ behind. The in-plane resolution is 1.5 mm, and the slice thickness is 5 mm. The same imaging routine was used for all measurements in order to keep systematic errors arising from the sequence design constant. All relevant measurement parameters are displayed in table 1.

For the velocity measurements, the M_1 encoding was set to $M_1^{enc} = 7.5\,\mathrm{mT/m{\cdot}ms^2}$ which corresponds to a maximum measurable velocity without phase aliasing of $v_{enc} = 1.566\,\mathrm{m/s}$. The velocity field was measured 256 times and averaged. Besides the mentioned flow rates, a measurement without flow (flow-off) was performed to compensate for errors due to eddy currents.

For the turbulence quantification, five different velocity sensitivities were measured reaching from $M_1^{enc} = 10\,\mathrm{mT/m{\cdot}ms^2}$ to $M_1^{enc} = 30\,\mathrm{mT/m{\cdot}ms^2}$, which were averaged 250 times for the highest and 150 times for the lowest M_1^{enc}. Multiple velocity sensitivities are required to resolve both high and low fluctuations in the velocity. For further details on the velocity and the RST measurements and data reconstruction, the reader is referred to Schmidt et al. (2021).

Measurements were performed at the MRI flow lab, which is part of the Institute of Fluid Mechanics at the University of Rostock. The laboratory is equipped with a 3 T whole-body MRI scanner (Magnetom Trio, Siemens Healthineers, Erlangen, Germany). The magnetic field gradients have a maximum strength of 40 mT/m gradient and 200 T/m/s slew rate.
The flow data was reconstructed from the MRV raw data using Matlab 2017a (The Mathworks, Natick, USA). The signal received from each of the 32 channels was combined using ESPIRiT, which is an eigenvalue approach for auto-calibrating the sensitivity of each coil (Uecker et al., 2014). For the velocity measurement, the phase angle obtained from the flow-off measurement was fitted onto Legendre polynomials of second degree and subtracted from the flow-on measurements to compensate for errors from eddy currents. Furthermore, known distortions due to rising magnetic field gradients at the outer edges of the FOV were corrected. Beyond that, no filters were applied to the data.

3. Results

Figure 2 shows the MRV results of the different stationary fluid samples. Signal intensity and phase angle show homogeneous distributions within the liquid-filled region for all mixtures. Only minor changes appear in the maximum values of the signal intensities, indicating that some of the samples lead to a higher signal-to-noise ratio (SNR). However, none of the samples shows significant changes compared to the others, indicating that for the selected components, water, glycerol, xanthan gum, and copper sulfate, the MRV results do not seem to depend on the mixing ratio. The total acquisition time for the measurement of flow velocity and RST in the sudden expansion of the FDA nozzle was 2 hours for each flow rate and flow medium. The whole measurement campaign was thus completed within one day. Figure 3 displays the results of velocity measurement for Q=501/min. As the geometry and the flow are axis-symmetric, only the upper half of the flow field is shown. Figure 4 depicts the distribution of shear stress $\dot{\gamma}$ calculated from the measured velocity field with plots of the dynamic viscosity measured for both fluids. One can see that at the occurring shear rates the viscosity of the non-Newtonian fluid is higher than in the Newtonian case. This hinders a direct comparison of the two flow fields based on the Reynolds numbers. Nevertheless, it can be concluded that in both fluids quantitative measurements with no apparent fluid-dependent errors are possible.

For the RST measurement, the differences in the flow fields of both fluids become more visible. Figure 5 displays the turbulent kinetic energy k calculated from the normal shear stress $\overline{u_z' u_z'}$ of the measured Reynolds stress tensor. The turbulence level in the Newtonian fluid is higher than in the non-Newtonian case. It is assumed that this manly arises from the mentioned differences in the viscosity at the present shear rates. The flow rate was set to reach a Reynolds number of 6500 for the Newtonian case. However, for the non-Newtonian case, the viscosity is significantly higher and thus the corresponding Reynolds number is smaller. Therefore, it is consistent that the turbulent kinetic energy is lower for the non-Newtonian case at the same volume flow rate. However, as both fluids were measured with the same M_1^{enc}, the encoding is considered to be not optimal for

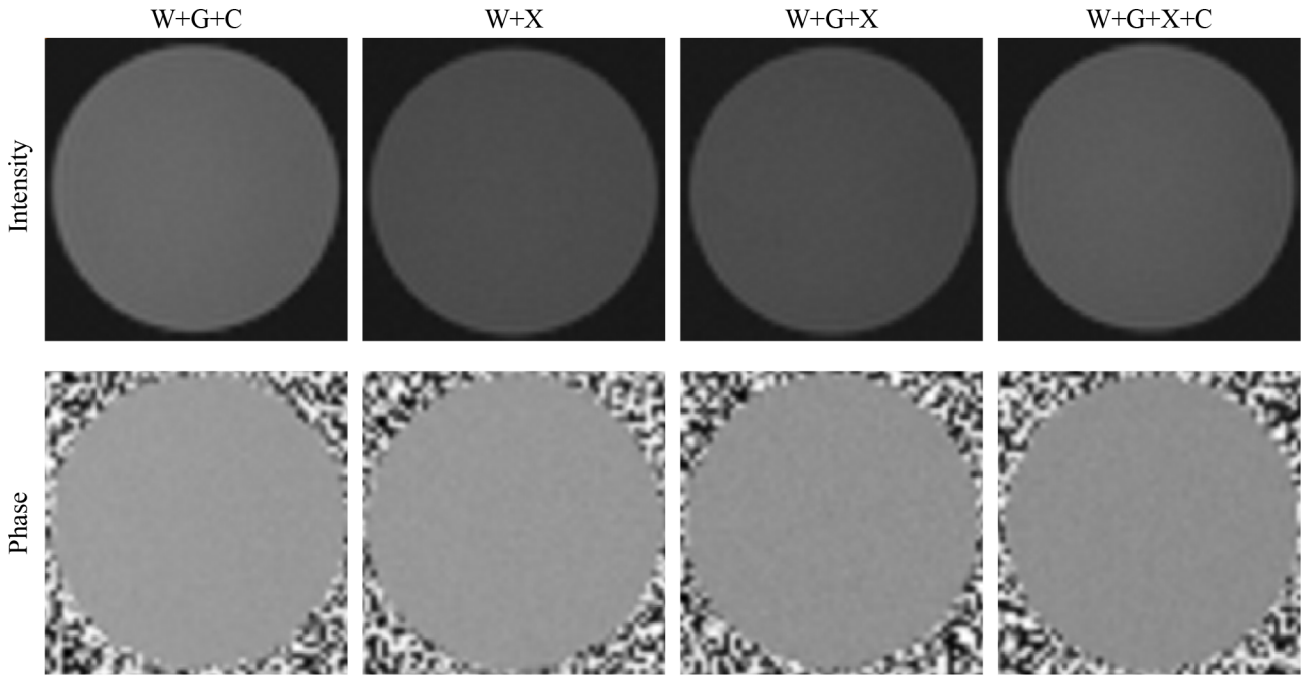

Figure 2. Results of 2D measurements in stationary fluid samples containing different mixtures of water (W), glycerol (G), xanthan gum (X), and copper sulfate (C). The top row shows the signal intensity, and the bottom row shows the resulting phase angle of a flow encoded measurement.

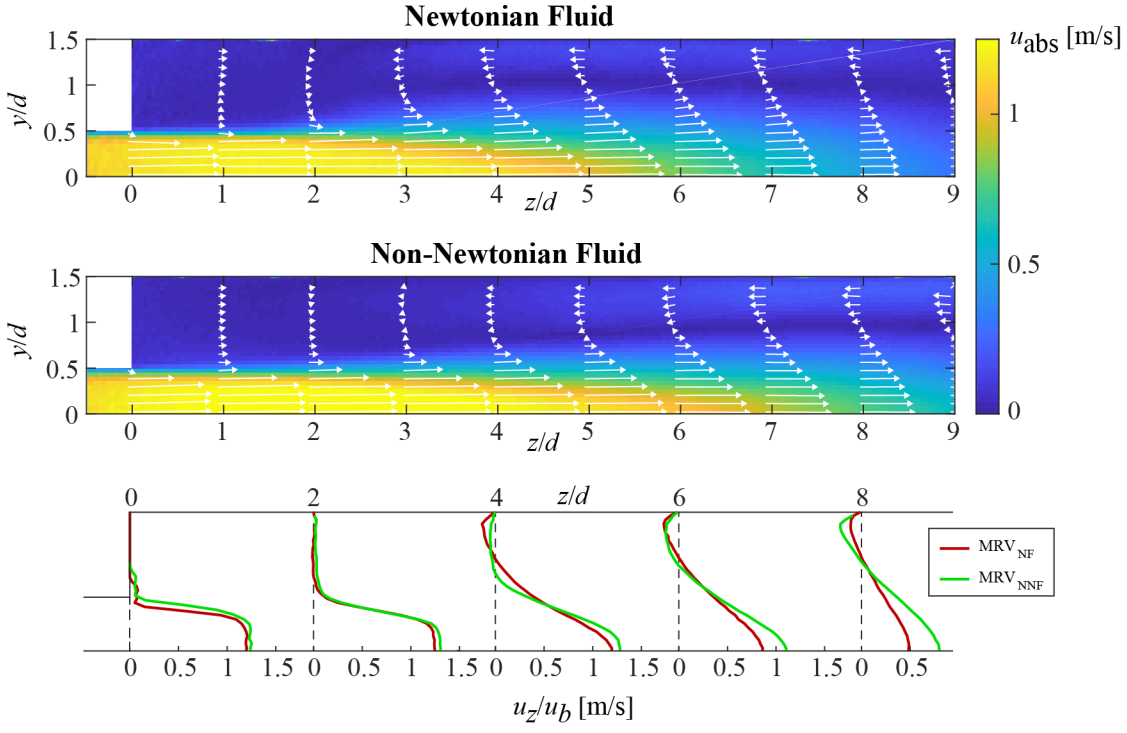

Figure 3. Measured Velocity field at flow rate 50 l/min in both Newtonian and non-Newtonian fluid. White arrows display in-plane velocity vector $\vec{u} = \{u_y, u_z\}$. The lower diagram shows the measured u_z velocity profiles for different axial positions.

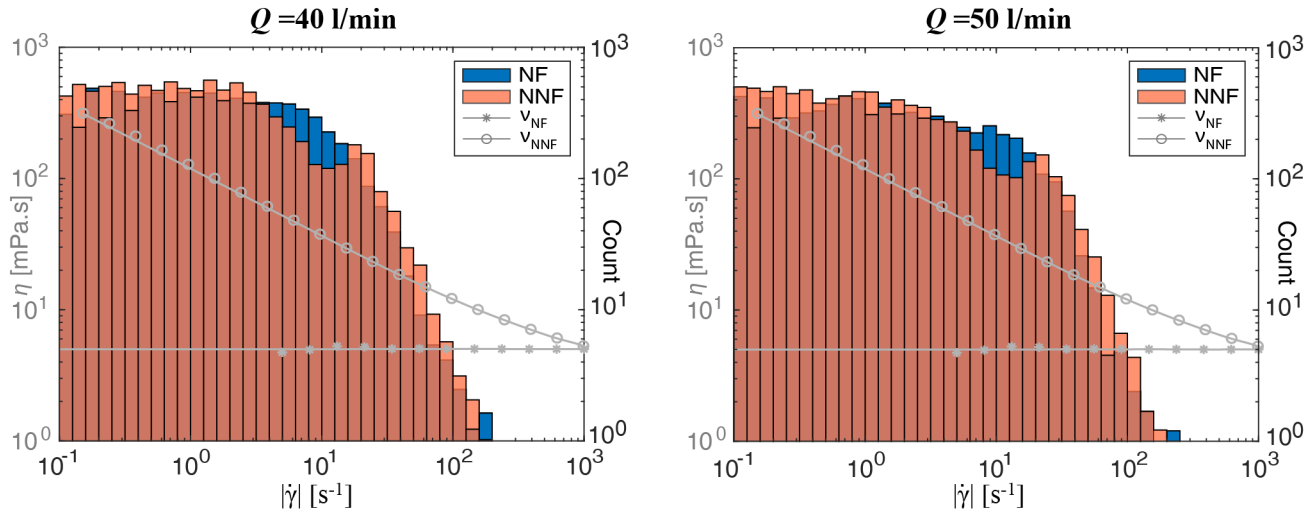

Figure 4. Histogram of shear stresses $\dot{\gamma} = \mathrm{d}u_z/\mathrm{d}y$ inside the FOV resulting from measured velocity field for Newtonian and non-Newtonian fluid at both measured flow rates. Additionally, kinematic viscosity $\nu = \eta/\rho$ for both fluids is displayed.

the non-Newtonian fluid. Please note, that this only affects the measurement uncertainty in the obtained results.

Moreover, fig. 5 exhibits significant qualitative differences in the distribution of turbulent kinetic energy. For example, the high turbulent kinetic energy region is located further downstream for the non-Newtonian fluid. From this, it can be assumed that the distribution of k strongly depends on the non-Newtonian effects. Neglecting them may lead to substantial errors in the prediction of non-Newtonian flows.

4. Discussion and Outlook

This study demonstrates the application of MRV in the FDA benchmark nozzle with a Newtonian and a shear-thinning fluid. No apparent influence of mixture-related errors was observed when measuring stationary samples of different Newtonian and non-Newtonian fluids. The velocity and RST data for two of the fluids was then captured in a two-dimensional slice at the sudden expansion of the FDA benchmark nozzle and showed promising results. Once the set up was installed, measurements for the different fluids could be performed with relatively little experimental effort for different flow rates. This shows that MRV is a promising method to provide comprehensive experimental data to investigate the influence of non-Newtonian effects on the flow field at several flow states comparatively quickly.

The same measurement procedure was used for all measurements to keep the influence of systematic errors arising from the encoding constant. From the calculated shear rates and the measured viscosity, it appears that the Reynolds number is much lower in the non-Newtonian fluid. Therefore, higher M_1^{enc} would have been required for the non-Newtonian case to capture the smaller

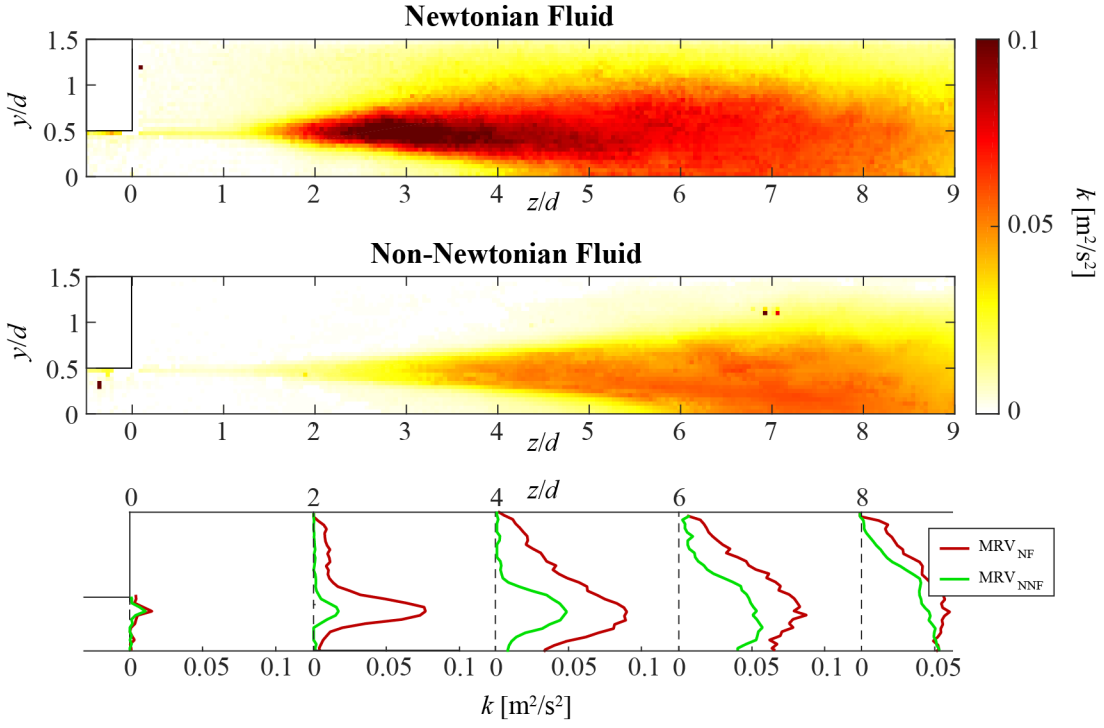

Figure 5. Contour plots and quantitative comparison of turbulent kinetic energy.

velocity fluctuations better. However, this only effects the measurement uncertainty and can be easily improved by increasing the M_1^{enc} in future measurements.
The qualitative differences in the distribution of the turbulent kinetic energy indicate that comprehensive experimental studies on the influence of non-Newtonian effects are needed. Further work will focus on the comparability of measurements in Newtonian and non-Newtonian fluids in terms of similar Reynolds numbers. In addition, comparison with the results of computational fluid dynamics is intended to study the effect of different viscosity models. To achieve this, work is also being done on the composition of fluids that exhibit certain non-Newtonian behavior and extending the study to a wider Reynolds numbers range.

Acknowledgements

The authors would like to acknowledge Sebastian Schmitter (Physikalisch-Technische Bundesanstalt (PTB), Braunschweig und Berlin, Germany; German Cancer Research Center (DKFZ), Medical Physics in Radiology, Heidelberg), and Simon Schmidt (University of Minnesota, Center for Magnetic Resonance Research, Minneapolis, USA; German Cancer Research Center (DKFZ), Medical Physics in Radiology, Heidelberg) for their support in the implementation of the MRV methods. Furthermore, we would like to thank Philip Töllner (Chair of Microfluidics, University of Rostock, Germany) for performing the viscosity measurements.

Nomenclature

d	contraction diameter
D	pipe diameter
k	turbulent kinetic energy [m^2/s^2]
M_1	first moment of the magnetic field gradient [$mT/m{\cdot}ms^2$]
M_1^{enc}	M_1 encoding [$mT/m{\cdot}ms^2$]
Q	flow rate [m^3/s]
TE	echo time [s]
TR	repetition time [s]
u_{abs}	absolute mean velocity
u_{b}	bulk velocity [m/s]
u_i	mean velocity [m/s]
u_i'	velocity fluctuation [m/s]
v_{enc}	velocity encoding [m/s]
$\dot{\gamma}$	shear stress[1/s]
η	dynamic viscosity [Pa·s]
μ	kinematic viscosity [m^2/s]
ρ	density [kg/m^3]

References

Haraldsson, H., Kefayati, S., Ahn, S., Dyverfeldt, P., Lantz, J., Karlsson, M., … Saloner, D. (2018). Assessment of reynolds stress components and turbulent pressure loss using 4d flow mri with extended motion encoding. *Magnetic resonance in medicine*, *79*(4), 1962–1971.

Hariharan, P., Giarra, M., Reddy, V., Day, S. W., Manning, K. B., Deutsch, S., … others (2011). Multilaboratory particle image velocimetry analysis of the fda benchmark nozzle model to support validation of computational fluid dynamics simulations. *Journal of biomechanical engineering*, *133*(4).

Hussein, B. K., Al-Azawy, M. G., Al-Waaly, A. A., & Hamza, Z. A. (2021). Evaluation of turbulence and non-newtonian blood rheology models through an fda nozzle. In *2021 international conference on advance of sustainable engineering and its application (icasea)* (pp. 1–5).

John, K., Wüstenhagen, C., Schmidt, S., Schmitter, S., Bruschewski, M., & Grundmann, S. (2022). Reynolds stress tensor and velocity measurements in technical flows by means of magnetic resonance velocimetry. *tm-Technisches Messen*, *89*(3), 201–209.

Konnigk, L., Torner, B., Bruschewski, M., Grundmann, S., & Wurm, F.-H. (2021). Equivalent scalar stress formulation taking into account non-resolved turbulent scales. *Cardiovascular Engineering and Technology*, *12*(3), 251–272.

Markl, M., Frydrychowicz, A., Kozerke, S., Hope, M., & Wieben, O. (2012). 4d flow mri. *Journal of Magnetic Resonance Imaging*, *36*(5), 1015-1036.

Schmidt, S., John, K., Kim, S. J., Flassbeck, S., Schmitter, S., & Bruschewski, M. (2021). Reynolds stress tensor measurements using magnetic resonance velocimetry: expansion of the dynamic measurement range and analysis of systematic measurement errors. *Experiments in Fluids*, *62*(6), 1–17.

Stewart, S. F., Hariharan, P., Paterson, E. G., Burgreen, G. W., Reddy, V., Day, S. W., ... others (2013). Results of fda's first interlaboratory computational study of a nozzle with a sudden contraction and conical diffuser. *Cardiovascular Engineering and Technology*, *4*(4), 374–391.

Trias, M., Arbona, A., Massó, J., Miñano, B., & Bona, C. (2014). Fda's nozzle numerical simulation challenge: non-newtonian fluid effects and blood damage. *PloS one*, *9*(3), e92638.

Uecker, M., Lai, P., Murphy, M. J., Virtue, P., Elad, M., Pauly, J. M., ... Lustig, M. (2014). Espirit—an eigenvalue approach to autocalibrating parallel mri: where sense meets grappa. *Magnetic resonance in medicine*, *71*(3), 990–1001.

Wapler, M. C., Leupold, J., Dragonu, I., von Elverfeld, D., Zaitsev, M., & Wallrabe, U. (2014). Magnetic properties of materials for mr engineering, micro-mr and beyond. *Journal of magnetic resonance*, *242*, 233–242.

Zwart, N. R., & Pipe, J. G. (2013). Multidirectional high-moment encoding in phase contrast mri. *Magnetic resonance in medicine*, *69*(6), 1553–1563.